Geophysical Research Letters

RESEARCH LETTER
10.1029/2022GL101075

**Key Points:**

- Tropical upwelling 10–5 hPa increased up to 30% from 2005 to 2021, increasing upper stratospheric $N_2O$ and reactive nitrogen production
- Increased upwelling is connected to stronger and more frequent Quasi-Biennial Oscillation easterlies at 10 hPa and above
- Increased upwelling changed $NO_x$-driven $O_3$ losses, increasing tropical $O_3$ from 15 to 7 hPa while reducing Arctic $O_3$ from 15 to 2 hPa

**Supporting Information:**

Supporting Information may be found in the online version of this article.

**Correspondence to:**

S. E. Strahan,
susan.strahan@nasa.gov

**Citation:**

Strahan, S. E., Coy, L., Douglass, A. R., & Damon, M. R. (2022). Faster tropical upper stratospheric upwelling drives changes in ozone chemistry. *Geophysical Research Letters*, *49*, e2022GL101075. https://doi.org/10.1029/2022GL101075

Received 1 SEP 2022
Accepted 15 OCT 2022

**Author Contributions:**

**Conceptualization:** Susan E. Strahan, Anne R. Douglass
**Data curation:** Megan R. Damon
**Formal analysis:** Susan E. Strahan
**Funding acquisition:** Susan E. Strahan
**Investigation:** Susan E. Strahan, Lawrence Coy, Anne R. Douglass
**Methodology:** Susan E. Strahan
**Resources:** Megan R. Damon
**Software:** Susan E. Strahan, Megan R. Damon
**Visualization:** Susan E. Strahan
**Writing – original draft:** Susan E. Strahan
**Writing – review & editing:** Susan E. Strahan, Lawrence Coy, Anne R. Douglass



# Faster Tropical Upper Stratospheric Upwelling Drives Changes in Ozone Chemistry

**Susan E. Strahan[1,2], Lawrence Coy[2,3], Anne R. Douglass[2], and Megan R. Damon[2,3]**

[1]GESTAR II, University of Maryland, Baltimore County, Baltimore, MD, USA, [2]NASA Goddard Space Flight Center, Greenbelt, MD, USA, [3]Science Systems and Applications, Inc., Lanham, MD, USA

**Abstract** Tropospheric trends in long-lived source gases $N_2O$ and the chlorofluorocarbons cause trends in $O_3$ through changes in their reactive product gases. Transport affects the product gases because it controls the distribution of the long-lived source gases. We find that large changes in tropical upwelling 10–5 hPa since 2012 have strengthened the northern branch of the upper stratospheric (UpS) transport circulation, dramatically altering the abundances of $N_2O$ and its odd nitrogen product gases, $NO_x$ and $HNO_3$. Increased upwelling is connected to stronger and more frequent Quasi-Biennial Oscillation easterly winds at 10 hPa and above. We use simulations with and without time varying MERRA2 meteorology to quantify the impact of dynamical changes on $O_3$ loss via the $NO_x$ and $ClO_x$ cycles. We find that dynamical impacts on these cycles explain the mid-stratospheric tropical $O_3$ increase and Arctic UpS $O_3$ decrease since 2005.

**Plain Language Summary** Changes in the upper stratospheric circulation over the past decade have altered composition between 30 and 40 km altitude. In the tropics, faster ascent carried greater amounts of nitrous oxide ($N_2O$), a gas produced at the surface, to the upper stratosphere. This increased the amount of the ozone-destroying nitrogen radicals produced from $N_2O$. Most of the extra nitrogen radicals traveled to the Arctic above ~32 km, where they increased ozone destruction. Below the altitude where the radicals are produced (about 35 km), the faster tropical ascent carries reduced amounts of nitrogen radicals to the middle stratosphere (~26 to 35 km), leading to an ozone increase. Observations by satellite instruments revealed changes in the composition. Model simulations showed that circulation change caused the composition changes that affected ozone. The circulation change was connected to changes in the tropical winds that circulate around the globe and change from easterly to westerly on a fairly regular basis. During the last 10 years, this long-standing pattern changed. This could be variability or the start of a trend; it's too soon to tell. Either way, it complicates the identification and attribution of the ozone increases we expect due to international treaties that banned the use of manmade chlorocarbons.

## 1. Introduction

Total column $O_3$ trends are used to identify ozone layer recovery and assess the Montreal Protocol's impact, but attributing their cause can be difficult because many processes affect $O_3$ and the process balance changes with altitude. Below 28 km, $O_3$ is predominantly controlled by transport because of its relatively long photochemical lifetime, but above, chemistry becomes increasingly important (Chipperfield et al., 1994). Gas phase stratospheric $O_3$ loss from 50 to 2 hPa (20–44 km) is predominantly controlled by the chemically reactive chlorine and nitrogen families, $ClO_x$ (Cl, $Cl_2$, ClO, $(ClO)_2$, OClO, and HOCl) and $NO_x$ (NO, $NO_2$, $NO_3$, and $N_2O_5$) (Brasseur et al., 1999). $NO_x$ is responsible for 50%–80% of $O_3$ loss from ~30 to 5 hPa but decreases in importance above as loss by $ClO_x$ increases to 30%–40% near 2 hPa; loss by $HO_x$ dominates above 2 hPa. Nitrous oxide ($N_2O$), emitted at the surface, reacts with $O^1D$ in the tropical middle and upper stratosphere and is the primary source of $NO_x$. $NO_y$ is the sum of reactive ($NO_x$) and reservoir nitrogen species ($HNO_3$ and $ClONO_2$); it behaves like a long-lived trace gas. Chlorofluorocarbons (CFCs), emitted at the surface and photolyzed in the stratosphere, are the primary sources of $ClO_x$. Most of the chlorine released forms the relatively unreactive reservoir species, HCl and $ClONO_2$, which then become sources for $ClO_x$ radicals involved in ozone loss cycles.

Tropospheric trends in long-lived source gases cause trends in $O_3$ through changes in their reactive product gases. Stratospheric $O_3$ is expected to increase because chlorine from manmade chlorocarbons has been declining at ~5%/decade since 2000 due to the Montreal Protocol (Engel et al., 2018), but the 3.0%/decade increase in tropospheric $N_2O$ (Lan et al., 2020) offsets some of that increase; stratospheric cooling reduces $O_3$ loss by $NO_x$,

partially mitigating the impact of increased $N_2O$ (Rosenfield & Douglass, 1998). At 2 hPa where $O_3$ loss by Cl peaks, Steinbrecht et al. (2017) report tropical and midlatitude $O_3$ from 2000 to 2016 increased at 1.5%/decade and 2.5%/decade, respectively. Chemistry climate model (CCM) studies attribute positive upper stratospheric (UpS; ∼10 to 1 hPa) $O_3$ trends to decreasing ozone depleting substances and cooling from increased $CO_2$ (Li et al., 2009; Shepherd & Jonsson, 2008).

While the source gases' tropospheric trends influence $NO_x$ and $ClO_x$ product gas trends, transport also plays an important role because it controls the distribution of the long-lived source gases that form radicals (Douglass et al., 2004); this affects $O_3$. For example, the vertical transport of $NO_y$ above 30 km, modulated by the Quasi-Biennial Oscillation (QBO), was shown to affect $O_3$ levels by modulating loss by $NO_2$ (Chipperfield et al., 1994; Zawodny & McCormick, 1991). Further, unidentified dynamical variations that decreased tropical $N_2O$ in the mid-stratosphere prior to 2014 were linked to increased $NO_x$ and decreased $O_3$ (Galytska et al., 2019; Neholuha et al., 2015). While ∼55% of $N_2O$ destruction occurs above 10 hPa, ∼70% of chlorocarbon destruction occurs below 10 hPa (Figure S1 in Supporting Information S1). Changes in tropical upwelling above 10 hPa therefore have a greater impact on the production and distribution of $NO_x$ than on $ClO_x$.

In this paper we show that the chemical impacts of recent dynamical changes shifted the balance of $O_3$ loss processes in the middle and upper stratosphere. The Microwave Limb Sounder (MLS) on Aura and the Atmospheric Chemistry Experiment Fourier Transform Spectrometer (ACE) on SCI-SAT have measured stratospheric composition since 2004 and 2003, respectively. We use their records of $N_2O$, $HNO_3$, $NO_x$, and $O_3$ over a 16-year period to examine how changes in reactive nitrogen species affected gas phase ozone chemistry above 30 hPa between June 2013 and May 2021 compared to the previous 8 years, June 2005–May 2013; we call this the quasi-decadal (QD) change. We use simulations of the Global Modeling Initiative (GMI) chemistry transport model (CTM) to understand how dynamical changes affected $O_3$ loss processes. We also identify the QBO's role in UpS circulation and composition.

## 2. Data and Model Experiments

We investigate UpS $O_3$ changes between June 2005 and May 2021 using MLS v5.0 Level 3 pressure level measurements of $O_3$, $HNO_3$, $N_2O$, and temperature (Livesey, Read, Wagner, et al., 2021). MLS $N_2O$ v5.0 data (190 GHz) have a negative drift of up to 10%/decade at 22 hPa and below but have no statistically significant drifts in the middle and upper stratosphere 50°S–50°N up to ∼3 hPa (Livesey, Read, Froidevaux, et al., 2021). Livesey, Read, Froidevaux, et al. (2021) found no evidence for drift in the $HNO_3$, $O_3$, and temperature records between 2005 and 2019. We use ACE v4.1 pressure level measurements of $NO_2$, NO, and $N_2O_5$ to calculate $NO_x$ (Boone et al., 2020); see SI for details. The ACE products used here are zonal monthly mean sunrise and sunset data averaged over 5° latitude bands. MERRA2 zonal ($u$) and meridional ($v$) winds, temperature, and vertical velocity omega ($dp/dz$) (Gelaro et al., 2017; Global Modeling and Assimilation Office [GMAO], 2015) were used to calculate the residual mean circulation velocities, $v^*$ and $w^*$ (Andrews et al., 1987). The residual mean circulation was then used to link trace gas changes to circulation changes.

The purpose of our model experiments is to separate the expected $O_3$ changes due to tropospheric source gas trends from dynamical changes that affected $O_3$ by altering source and product gas distributions and hence the balance of $O_3$ production and loss. To this end we integrated 2 GMI CTM simulations for June 2005 to May 2021 with the same source gas boundary conditions (e.g., for $N_2O$, CFCs, $CH_4$, etc.) but with different meteorological fields (Strahan et al., 2013). The Baseline simulation uses MERRA2 fields for 2005–2021, while the Fixed Dynamics experiment ("FixDyn") begins with the same initial conditions as Baseline but recycles MERRA2 fields from June 2005 to May 2007 until the end of the run in May 2021. Thus, the FixDyn simulation has no long-term dynamical trend while still generating the two largest sources of stratospheric transport variability: the annual cycle of the Brewer Dobson circulation (BDC) and the QBO. This particular 2-year period was chosen because the MERRA2 tropical winds from ∼100 to 3 hPa on 1 June 2005, are similar to those on 1 June 2007 (i.e., QBO has the same phase), minimizing the adjustment to tropical transport from recycling. June is a good transition month for recycling because planetary wave activity is at a minimum, which minimizes extratropi-

cal transport adjustments. Both simulations are integrated with 1° × 1.25° horizontal resolution on 72 hybrid sigma-pressure levels, use the same chemical mechanism, have the same solar cycle, and have the same tropospheric emissions. All simulated and observed annual means are calculated from June to the following May. QD changes are the difference between the average of June 2013–May 2021 and June 2005–May 2013; the mean difference between these periods is 8 years.

With its realistic representation of 2005–2021 meteorology, Baseline's QD changes in stratospheric composition are very similar to those observed (Sections 3 and 4), allowing us to explain the observed $O_3$ changes in terms of changes in loss processes. Comparisons of the QD changes in loss processes in Baseline and FixDyn identify where key dynamical changes occurred that altered the loss processes and the expected $O_3$ changes.

## 3. Quasi-Decadal Changes $N_2O$, $NO_y$, and Dynamics

Odd nitrogen produced from $N_2O + O^1D$ is mostly found as $HNO_3$ below ∼15 hPa and as $NO_x$ above. Figure 1a shows QD increases greater than 10% in MLS $N_2O$ throughout the UpS where the $O^1D$ reaction is important; QD increases exceed 15% over large regions. Froidevaux et al. (2022) noticed large increases of >1%/year in 50°S–50°N UpS $N_2O$. The pattern of simulated QD $N_2O$ changes in GMI Baseline matches the observations well (Figure 1b). The known negative MLS $N_2O$ drift below 20 hPa likely contributes to the negative changes there, but the simulation suggests that they are qualitatively correct. Our analysis focuses on changes 20–3 hPa, where the $N_2O$ drift is insignificant. In the polar regions above 7 hPa where $N_2O$ is <30 ppb and both MLS and GMI show changes >10%, small differences between GMI and MLS mixing ratios can lead to large differences in their QD percentage changes (see Figure S2 in Supporting Information S1).

The increased $N_2O$ also leads to increased $HNO_3$ above 5 hPa at most latitudes that is in excess of the $N_2O$ tropospheric growth rate of 2.4%/8 years (white contours in Figure 1); the greatest $HNO_3$ increases are found north of 50°N and extend down to ∼10 hPa. Low $HNO_3$ mixing ratios at 3 hPa increase the uncertainty of the percentage change (Figure S2 in Supporting Information S1). In the tropics 20–7 hPa, QD $N_2O$ increases while QD $HNO_3$ and $NO_x$ (Figures 1c and 1e) decrease, indicating these are transport controlled changes consistent with increased upwelling (i.e., younger air containing higher $N_2O$ and lower $NO_y$). In the Arctic, simulated and observed $NO_x$ and $HNO_3$ changes exceed source gas growth above 10 hPa while in the Antarctic they do not (Figure 1f). Figure S3 in Supporting Information S1 shows simulated QD $NO_x$ and $NO_y$ changes at all latitudes. Increases in UpS $NO_y$ are smaller than those of $N_2O$ because the net $NO_y$ increase depends on both production and transport, and increased upwelling reduces $NO_y$ transported to the UpS.

Figure 2 demonstrates the dynamical connection between changes in the UpS circulation and increased $N_2O$ and $NO_y$. The Baseline simulation shows a net increase in tropical $NO_y$ production that peaks near 5 hPa, paralleling the large QD increases in $N_2O$ (Figure 2a). The comparison with annual mean MERRA2 tropical vertical velocities ($w^*$) in Figure 2b reveals the cause. Both the observed and simulated $N_2O$ annual means from 2005 to 2021 change in near lock step with the MERRA2 $w^*$ at 7 hPa; years with stronger upwelling increase UpS $N_2O$. Similarly strong correlations between MLS $N_2O$ and $w^*$ are found between 10 and 3 hPa (Figure S4 in Supporting Information S1). Figure 2c shows QD changes in the UpS residual circulation. There are large increases in the tropical ascent ($w^*$) and the poleward meridional velocity in both hemispheres, and the northern hemisphere (NH) $v^*$ increases ∼8 to 5 hPa are more than double those in the southern hemisphere (SH), much like the $NO_x$ changes in Figure 1f. The large UpS QD increase in $w^*$ is driven by increased ascent rates in SH winter months (Figure S5 in Supporting Information S1). Along with the QD temperature changes (Figure 2d), the $w^*$ and $v^*$ changes indicate strengthening of northern branch of the UpS BDC. Similar circulation changes, along with related lower stratospheric (LS) $N_2O$ changes, were identified in four different reanalysis driven simulations of 2005–2017 (Ploeger & Garny, 2022). Large NH $v^*$ changes are consistent with elevated $HNO_3$ and $NO_x$ in the Arctic.

The QBO's role in the UpS composition change is shown in Figures 2e and 2f. Because increased tropical vertical velocities and cooling are dynamical responses to the tropical easterly zonal wind shear (Baldwin et al., 2001), a correlation is also expected between $N_2O$ and the zonal wind. Figure 2e shows monthly mean MLS $N_2O$ and MERRA2 zonal wind ($u$) at 7 hPa over the 2005–2021 period. Their correlation is −0.7 and higher $N_2O$ values

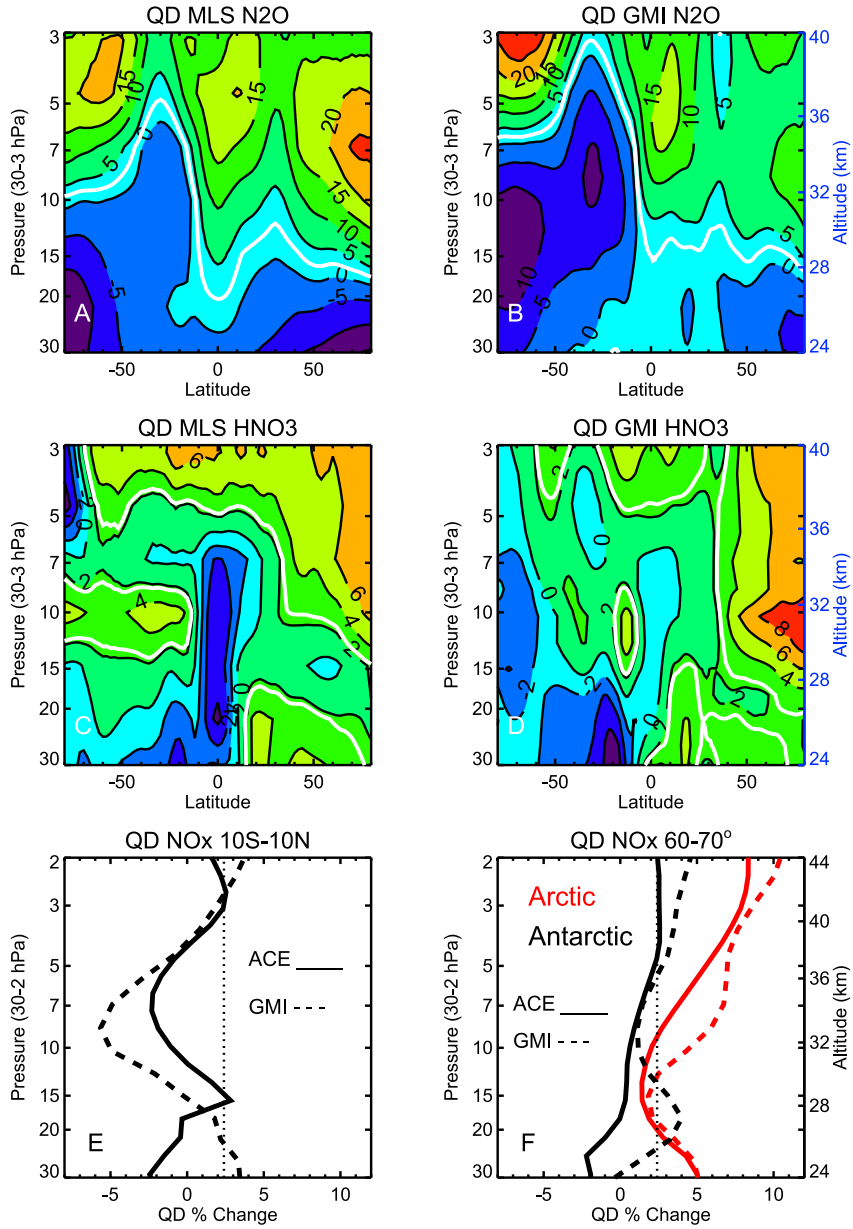


**Figure 1.** Quasi-decadal (QD) percentage changes in (a) Microwave Limb Sounder (MLS) $N_2O$, (b) Global Modeling Initiative (GMI) Baseline $N_2O$, (c) MLS $HNO_3$, (d) GMI Baseline $HNO_3$, (e) tropical ACE and GMI Baseline $NO_x$, and (f) same as (e) except for the Arctic and Antarctic, 60°–70°. White contour value, 2.4, is the tropospheric source gas growth.

are associated with strong easterly winds, consistent with $N_2O$ and $w^*$ from 10 to 3 hPa (Figure S4 in Supporting Information S1). QD changes in the tropical zonal wind are consistent with the increased $w^*$ from 2013 to 2021. Figure 2f shows MERRA2 10°S–10°N zonal wind probability distributions at 7 hPa for 2005–2013 and 2013–2021. The most probable zonal wind went from −3 m/s in the early period to −32 m/s in the later period. In the early period, winds were weakly easterly 66% of the time (mean wind −6 m/s) while in the later period they were easterly 79% of the time (mean wind −14 m/s). QD changes in the tropical UpS zonal wind (i.e., the QBO) drove mean upwelling changes that increased tropical and NH $N_2O$ and $NO_y$. The annual mean MERRA2 zonal winds at 2°S and the Singapore wind data record (1.3°S) at 10 hPa (the lowest pressure available) agree very well between 1995 and 2021, as do QD changes in the wind speed distributions 2005–2021, based on monthly mean data (Figure S6 in Supporting Information S1). The MERRA2 zonal winds averaged 10°S–10°N have the same behavior as MERRA2 2°S winds but are typically 0–5 m/s more easterly.

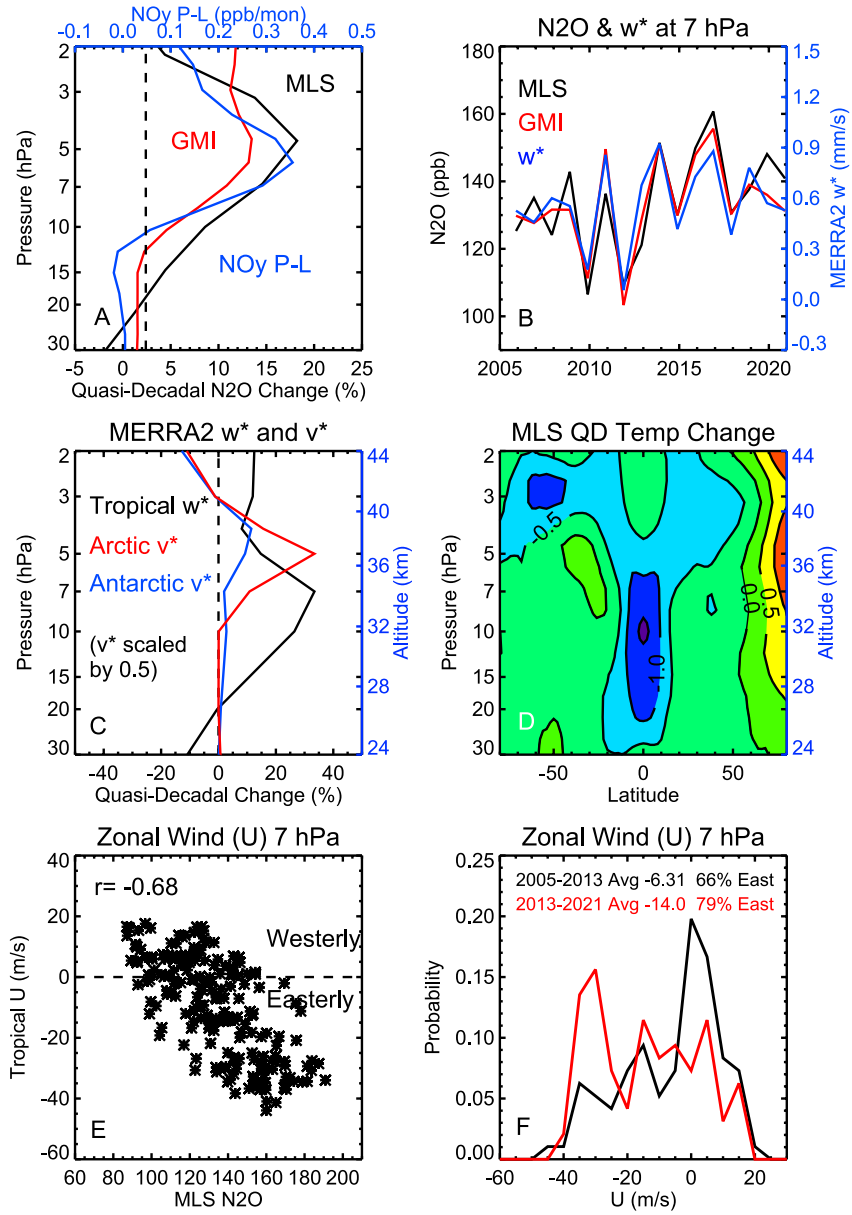


**Figure 2.** (a) Quasi-decadal (QD) percentage change in Microwave Limb Sounder (MLS) and Global Modeling Initiative (GMI) Baseline 10°S–10°N $N_2O$ profiles and simulated QD change in Baseline net odd nitrogen production-loss (P-L) in ppb/month. (b) Annual mean MLS and Baseline $N_2O$ for 2005–2021 and MERRA2 vertical velocities ($w$*) at 7 hPa 10°S–10°N. (c) QD percentage changes in MERRA2 $w$* profiles 10°S–10°N (black), and $v$* profiles for the Arctic (50°–70°N, red), and Antarctic (50°–70°S, blue). (d) QD MLS global temperature change (K). (e) MERRA2 monthly zonal mean zonal wind ($u$) and MLS monthly zonal mean $N_2O$, 7 hPa 10°S–10°N. (f) Probability distributions of MERRA2 10°S–10°N zonal winds for June 2005–May 2013 (black) and June 2013–May 2021 (red).

## 4. Dynamically Driven Changes in $O_3$ Loss Cycles and $O_3$ Impacts

We explore the impacts of the UpS $NO_y$ changes on ozone using two dynamically different GMI simulations: Baseline, with MERRA2 meteorology for 2005–2021, and FixDyn, which repeats the June 2005–May 2007 MERRA2 meteorology for the entire 16-year period. Since both simulations are forced by the same source gas surface boundary conditions for $N_2O$, $CH_4$, and the halocarbons, the differences between them show the effects of dynamically driven composition change on $O_3$ between 2005 and 2021.

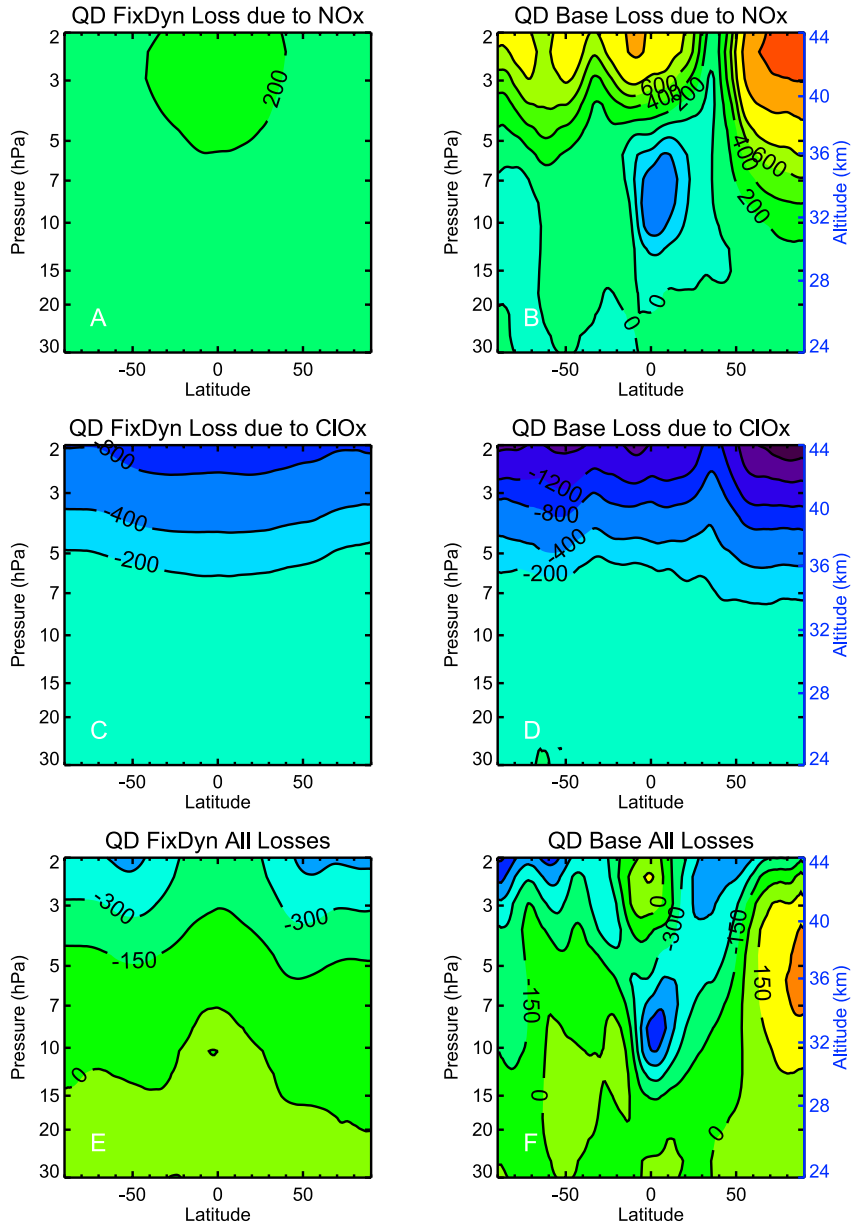


**Figure 3.** Quasi-decadal (QD) Changes in $O_3$ loss (in ppb/mon) due to (a) FixDyn $NO_x$, (b) Baseline $NO_x$, (c) FixDyn $ClO_x$, and (d) Baseline $ClO_x$. QD Change in $O_3$ loss (ppb/mon) from all $O_3$ loss cycles for (e) FixDyn and (f) Baseline.

$NO_x$ and $ClO_x$ radicals account for most gas phase $O_3$ loss from 50 to 2 hPa (Figure S7 in Supporting Information S1) and changes in their abundances strongly influence $O_3$. Figure 3 contrasts the QD $O_3$ loss changes in Baseline and FixDyn simulations caused by $NO_x$, $ClO_x$, and the total of all radical families, which includes $HO_x$, $O_x$, and $BrO_x$. (Losses shown as positive numbers.) FixDyn shows a small, hemispherically symmetric increase in loss by $NO_x$ in the tropical UpS, expected due to the source gas trend (Figure 3a). Baseline $O_3$ loss by $NO_x$ (Figure 3b) shows a pattern similar to the observed QD $HNO_3$ and $NO_x$ changes (Figure 1), with reduced tropical loss from ~20 to 7 hPa and greatly increased extratropical loss above 7 hPa, especially in the Arctic.

$O_3$ loss by $ClO_x$ increases with altitude while declining chlorocarbons reduce chlorine by ~5%/decade. The QD change in $O_3$ loss by $ClO_x$ is therefore negative and becomes more negative with altitude; this is seen in both simulations (Figures 3c and 3d). There is little hemispheric asymmetry compared to the QD change in $O_3$ loss by $NO_x$. This is due to the differences in the altitudes where $N_2O$ and chlorocarbon destruction occurs and to the altitudes with increased upwelling. Below 10 hPa, ~70% of Cl from chlorocarbons has already been released, thus

the impact of increased UpS upwelling has minor impact on $ClO_x$ production. In the Arctic UpS, Baseline QD $O_3$ loss by $ClO_x$ decreased by factors of 2–3 compared to FixDyn. This is consistent with observed and simulated QD declines in Arctic ClO at 3 hPa that is roughly twice the magnitude as all other latitudes (Figure S8 in Supporting Information S1). The large Arctic ClO decrease is cause by increased UpS $NO_x$, which reduces the ClO/Cl ratio and thus the $O_3$ loss by $ClO_x$ (Douglass et al., 1995).

The QD change in the sum of all $O_3$ losses is nearly equal to the losses from $NO_x$ and $ClO_x$ in both simulations (Figures 3e and 3f). QD losses by $HO_x$, $O_x$ and $BrO_x$ cycles, shown in Figure S9 in Supporting Information S1, are smaller than $ClO_x$ or $NO_x$ losses and look nearly the same in Baseline and FixDyn. The QD changes in all losses in both simulations are very small below 15 hPa, where transport influences $O_3$ more than chemistry. But unlike FixDyn, the spatial pattern and magnitudes of Baseline's QD change in total loss between 15 and 3 hPa is clearly dominated by changes in $NO_x$ losses from 20°S–80°N (Figure 3b).

Stratospheric $O_3$ changes depend on changes in production (P), loss (L), and transport, depending on the local $O_3$ lifetime. The QD $O_3$ P-L changes in both simulations, Figures 4a and 4b, look very much like the total loss changes in Figures 3e and 3f but with opposite sign (because loss is positive in Figure 3). The Baseline QD $O_3$ changes (Figure 4d) are in excellent agreement with the MLS observed changes (Figure 4f), and the pattern of changes in both look very much like the P-L changes, which are largely determined by changes in loss by $NO_x$ and $ClO_x$. These patterns are dramatically different from the FixDyn $O_3$ changes, which are due only to tropospheric source gas trends (Figure 4c).

Figure 4e shows QD $O_3$ changes caused only by the dynamically driven composition change: this is the difference between Baseline and FixDyn QD $O_3$ (Figures 4d–4c). The strong similarities between the patterns and magnitudes of MLS $O_3$ changes (Figures 4f) and 4e indicate that $O_3$ changes from 15 to 2 hPa during the 2005–2021 period were strongly influenced by dynamical changes that affected $O_3$ loss chemistry The dynamically driven chemical features include *a* >300 ppb increase in tropical middle stratospheric $O_3$ and small decreases in Arctic UpS $O_3$ that occur in spite of decreasing chlorine. Both changes are consistent with the positive tropical trend from 30 to 35 km and the near zero zonal mean Arctic trend at 35 km for 2004–2018 reported by Sofieva et al. (2021). Both the observations and simulation show QD $O_3$ decreases from 20° to 50°S, 20–7 hPa where the QD $O_3$ P-L is near zero. These $O_3$ decreases are likely due to transport rather than dynamically driven changes affecting loss families.

Figure 4g shows the QD changes in the 20–2 hPa $O_3$ column, which is largely controlled by gas phase photochemistry. FixDyn shows $O_3$ increases of ∼0.3 DU with little latitude variation. Baseline and MLS $O_3$ changes deviate from FixDyn at all latitudes except 30°–50°N. The increased upwelling that reduces losses by $NO_x$ explains the nearly 2 DU equatorial increase observed by MLS. From 60° to 80°N, MLS shows no increase in $O_3$, consistent with increased UpS loss by $NO_x$ that negates the recovery due to reduced chlorine. MLS also shows QD decreases 12°–40°S of 1/2 DU less than FixDyn; given the small changes in P-L this decrease is due mostly to transport. The observed and simulated 1 DU increase in the Antarctic is explained by decreased loss by $NO_x$ below 5 hPa (Figures 1f and 3b). The dynamically driven part column changes 20°S–20°N are 1.0 DU (=1.25 DU/decade), while total column tropical trends for 1997–2016 are not statistically different from zero (Braesicke et al., 2018). The UpS increase reported here and the lack of a tropical total column trend are both consistent with tropical vertical profile trends 1997–2017 that are positive in the UpS and negative in the LS (Petropavlovskikh et al., 2019).

## 5. Conclusions

We demonstrated that the observed $O_3$ changes in the tropical middle stratosphere and the Arctic UpS from 2005 to 2021 resulted from chemical changes caused by increased tropical upwelling. The upwelling changes are connected to the increased frequency and intensity of QBO easterly winds at 10 hPa and above that transported $N_2O$ to the UpS and increased $NO_y$ production. UpS $NO_y$ increased above ∼5 hPa and was transported largely to the Arctic, where it increased $O_3$ loss by $NO_x$ and prevented $O_3$ increase in the 20–2 hPa column 60°–90°N. Below ∼5 hPa, faster ascent reduced tropical $NO_y$, leading to an increase of ∼1 DU/decade in the 20–2 hPa $O_3$ column 20°S–20°N. These effects are significant in the context of current total column trend estimates 1997–2016 that are ≤1 DU/decade from 60°S to 60°N (Braesicke et al., 2018).

Decadal scale changes in the UpS circulation since 2005 changed odd nitrogen source and reservoir gas distributions in a way that changed the rate of $O_3$ recovery expected due to declining chlorine. This had little impact on

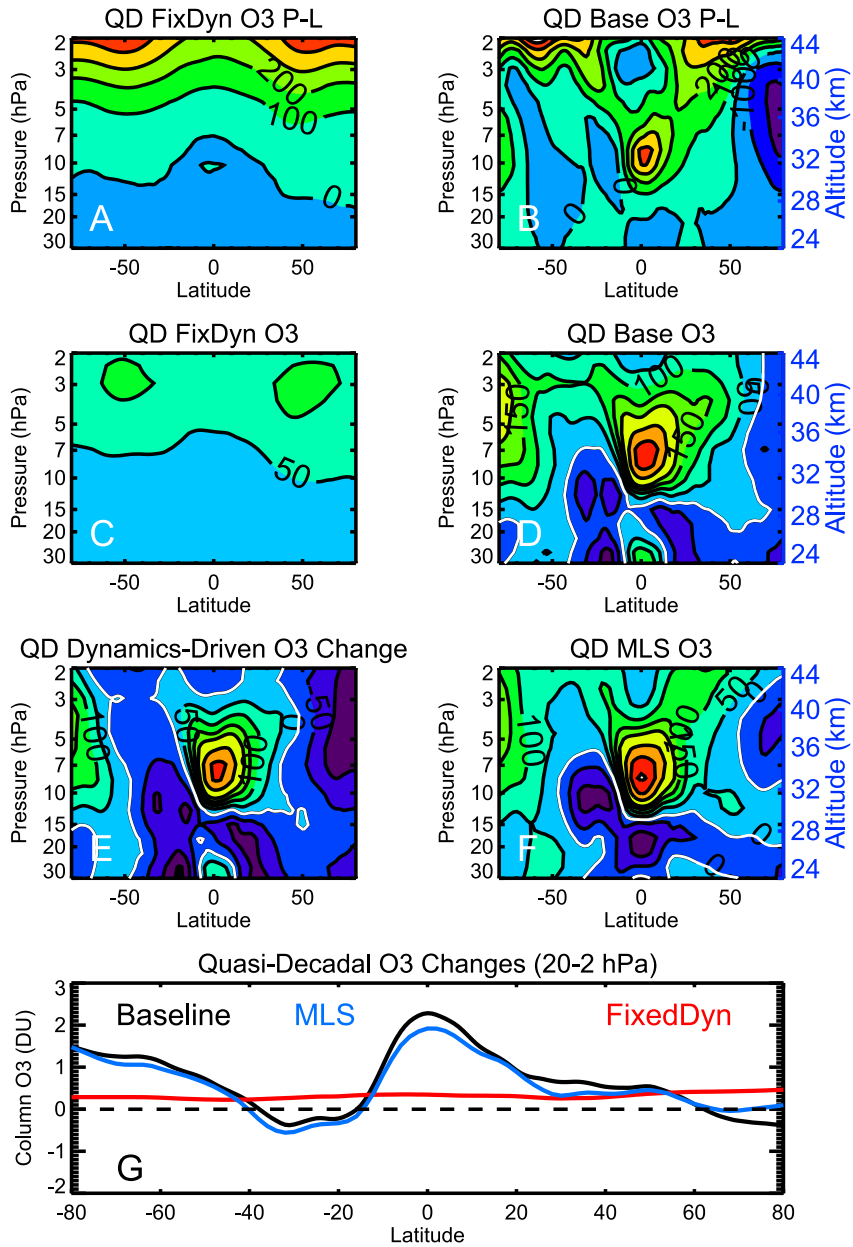


**Figure 4.** Quasi-decadal (QD) Changes in $O_3$ production-loss (P-L) in ppb/mon from 80°S to 80°N for (a) FixDyn and (b) Baseline. QD $O_3$ changes (ppb) for (c) FixDyn, (d) Baseline, (e) Baseline-FixDyn, and (f) Microwave Limb Sounder (MLS) $O_3$. (g) QD $O_3$ changes for the 20–2 hPa column for Baseline, MLS (blue), and FixDyn (red).

reactive chlorine because of differences in the altitudes where their respective source gases are destroyed. These effects contribute to UpS $O_3$ trends since 2005 and are likely not accounted for in trend calculations. Ozone trend regressions attempt to account for transport driven $O_3$ variability caused by the QBO using coefficients that reflect its LS phase (see Ch. 4 in Petropavlovskikh et al. (2019)). The QBO-related changes identified here are different because they occurred far above the LS, altered $O_3$ loss processes rather than $O_3$ transport, and occurred over a period much longer than a QBO cycle. This composition change will not have a quasi-biennial signature and a trend fit using LS QBO coefficients will not regress this variability.

CCMs are our primary tools for projecting future stratospheric $O_3$ abundances and most are able to internally generate a QBO. Gravity wave (GW) fluxes play a substantial role in maintaining the QBO, however, in most CCMs they are parameterized and tuned to match the observed, present-day QBO period and amplitude (Richter

et al., 2020). CCMs with parameterized GW and fixed GW sources are unable to change with the changing tropospheric climate, leading Richter et al. (2020) to conclude that this creates great uncertainty in the QBO's behavior in a future climate.

Several studies have shown that the 2016 and the 2019/2020 QBO disruptions were caused by large equatorward meridional momentum fluxes that penetrated the tropics (Antsey et al., 2021; Coy et al., 2017; Osprey et al., 2016). The Antsey et al. (2021) analysis of CCMs involved in the QBO Initiative (a model intercomparison) and of two recent QBO disruptions provides evidence that the QBO is likely to weaken and experience additional disruptions in a warming climate. They argue that several robust model responses to climate change, including the speed up of the BDC and the weakening of westward winds at the subtropical edges of the QBO, make the QBO more vulnerable to extratropical wave fluxes penetrating the tropics. An increased frequency of disruptions will make future stratospheric composition less predictable.

Neholuha et al. (2015) reported a circulation change of the opposite sign in the tropics (*i.e.*, slower ascent) from 1991 to 2013 that increased $NO_x$ and decreased $O_3$ ~15 to 7 hPa; the cause was not identified. The composition changes we report, which occurred between 2005 and 2021, also span more than a decade and both results may indicate a multi-decadal dynamical variation of unknown source. Regardless, it's clear that dynamical changes on decadal scales are able to significantly alter distributions of a chemical family, $NO_y$, whose radicals control a major stratospheric $O_3$ loss cycle. These changes, even if only decadal, have a measurable impact current $O_3$ trends.

## Data Availability Statement

Aura MLS version 5 data are available at http://mls.jpl.nasa.gov. ACE data are available through the following sign-up link: https://databace.scisat.ca/l2signup.php. The monthly mean Singapore zonal mean winds, derived from radiosonde data obtained by the Meteorological Service Singapore, are available at https://acd-ext.gsfc.nasa.gov/Data_services/met/qbo/QBO_Singapore_Uvals_GSFC.txt. The GMI simulations can be found at https://portal.nccs.nasa.gov/datashare/dirac/gmidata2/users/mrdamon/Hindcast-Family/HindcastMR2; see the HindcastMR2V2 and HindcastMR2V2-FixedDyn subdirectories. Model simulations were integrated with meteorological fields from the following collection, after reducing the horizontal resolution to 1° latitude by 1.25° longitude: GMAO (2015). This same data collection is the source for other MERRA2 products used in this study.

**Acknowledgments**
The authors thank Luke Oman (NASA GSFC) for calculating the MERRA2 residual vertical and meridional velocities. SES acknowledges research support from the NASA Atmospheric Chemistry Modeling and Analysis Program Grant 80NSSC19K1005 and thanks the NASA Modeling Analysis and Prediction program for model support. Resources supporting this work were provided by the NASA High-End Computing (HEC) Program through the NASA Advanced Supercomputing (NAS) Division at the Ames Research Center and the NASA Center for Climate Simulation (NCCS) at the Goddard Space Flight Center.

## References

Andrews, D. G., Holton, J. R., & Leovy, C. B. (1987). *Middle atmosphere Dynamics* (p. 489). Academic Press.

Antsey, J. A., Banyard, T. P., Butchart, N., Coy, L., Newman, P. A., Osprey, S., & Wright, C. J. (2021). Prospect of increased disruption to the QBO in a changing climate. *Geophysical Research Letters*, *48*(15), e2021GL093058. https://doi.org/10.1029/2021GL093058

Baldwin, M. P., Gray, L. J., Dunkerton, T. J., Hamilton, K., Haynes, P. H., Randel, W. J., et al. (2001). The Quasi-Biennial Oscillation. *Reviews of Geophysics*, *39*(2), 179–229. https://doi.org/10.1029/1999rg000073

Boone, C. D., Bernath, P. F., Cok, D., Jones, S. C., & Steffen, J. (2020). Version 4 retrievals for the Atmospheric Chemistry Experiment Fourier Transform Spectrometer (ACE-FTS) and imagers. *Journal of Quantitative Spectroscopy and Radiative Transfer*, *247*, 106939. https://doi.org/10.1016/j.jqsrt.2020.106939

Braesicke, P., Neu, J., Fioletov, V., Godin-Beekmann, S., Hubert, D., Petropavlovskikh, I., et al. (2018). Update on global ozone: Past present, and future. Chapter 3 in *Scientific assessment of ozone depletion: 2018*. (Global Ozone Research and Monitoring Project — Report No. 58). World Meteorological Organization.

Brasseur, G. P., Orlando, J. J., & Tyndall, G. S. (1999). *Atmospheric chemistry and global change* (p. 654). Oxford University Press.

Chipperfield, M. P., Gray, L. J., Kinnersley, J. S., & Zawodny, J. (1994). A two dimensional model study of the QBO signal in SAGE II $NO_2$ and $O_3$. *Geophysical Research Letters*, *21*(7), 589–592. https://doi.org/10.1029/94gl00211

Coy, L., Newman, P. A., Pawson, S., & Lait, L. R. (2017). Dynamics of the disrupted 2015/16 Quasi-Biennial Oscillation. *Journal of Climate*, *30*(15), 5661–5674. https://doi.org/10.1175/jcli-d-16-0663.1

Douglass, A. R., Schoeberl, M. R., Stolarski, R. S., Waters, J. W., Russell, J. M., III, Roche, A. E., & Massie, S. T. (1995). Interhemispheric differences in springtime production of HCl and $ClONO_2$ in the polar vortices. *Journal of Geophysical Research*, *100*(D7), 13967–13978. https://doi.org/10.1029/95jd00698

Douglass, A. R., Stolarski, R. S., Strahan, S. E., & Connell, P. S. (2004). Radicals and reservoirs in the GMI chemistry and transport model: Comparison to measurements. *Journal of Geophysical Research*, *109*(D16), D16302. https://doi.org/10.1029/2004JD004632

Engel, A., Rigby, M., Burkholder, J. B., Fernandez, R. P., Froidevaux, L., Hall, B. D., et al. (2018). Update on ozone-depleting substances (ODSs) and other gases of interest to the Montreal protocol. Chapter 1 in *Scientific assessment of ozone depletion: 2018* (Global Ozone Research and Monitoring Project — Report No. 58). World Meteorological Organization.

Froidevaux, L., Kinnison, D. E., Santee, M. L., Millan, L., Livesey, N. J., Read, W. G., et al. (2022). Upper stratospheric ClO and HOCl trends (2005–2020): Aura Microwave Limb Sounder and model results. *Atmospheric Chemistry and Physics*, *22*(7), 4779–4799. https://doi.org/10.5194/acp-22-4779-2022

Galytska, E., Rozanov, A., Chipperfield, M. P., Dhomse, S. S., Weber, M., Arosio, C., et al. (2019). Dynamically controlled ozone decline in the tropical mid-stratosphere observed by SCIAMACHY. *Atmospheric Chemistry and Physics*, *19*(2), 767–783. https://doi.org/10.5194/acp-19-767-2019

Gelaro, R., McCarty, W., Suarez, M. J., Todling, R., Molod, A., Takacs, L., et al. (2017). The Modern-Era Retrospective analysis for research and Applications, version 2 (MERRA-2). *Journal of Climate*, *30*(14), 5419–5454. https://doi.org/10.1175/jcli-d-16-0758.1

Global Modeling and Assimilation Office (GMAO). (2015). *MERRA-2 tavg3_3d_asm_Nv: 3d,3-hourly, time-averaged, model-level, assimilation, assimilated meteorological fields V5.12.4*. Goddard Earth Sciences Data and Information Services Center (GES DISC). https://doi.org/10.5067/SUOQESM06LPK

Lan, X., Tans, P., Hall, B. D., Dutton, G., Mühle, J., Elkins, J. W., & Vimont, I. (2020). Long-lived greenhouse gases [in "State of the Climate in 2020"]. *Bulletin of the American Meteorological Society*, *102*(8), S83–S87. https://doi.org/10.1175/BAMS-D-21-0098.1

Li, F., Stolarski, R. S., & Newman, P. A. (2009). Stratospheric ozone in the post-CFC era. *Atmospheric Chemistry and Physics*, *9*(6), 2207–2213. https://doi.org/10.5194/acp-9-2207-2009

Livesey, N., Read, W. G., Froidevaux, L., Lambert, A., Santee, M. L., Schwartz, M. J., et al. (2021). Investigation and amelioration of long-term instrumental drifts in water vapor and nitrous oxide measurements from the Aura Microwave Limb Sounder (MLS) and their implications for studies of variability and trends. *Atmospheric Chemistry and Physics*, *21*(20), 15409–15430. https://doi.org/10.5194/acp-21-15409-2021

Livesey, N., Read, W. G., Wagner, P. A., Froidevaux, L., Santee, M. L., Schwartz, M. J., et al. (2021). Earth Observing System (EOS) Aura Microwave Limb Sounder (MLS) version 5.0x level 2 and 3 data quality and description document. JPL D-105336 Rev A.

Neholuha, G. E., Siskind, D. E., Lambert, A., & Boone, C. (2015). The decline in mid-stratospheric tropical ozone since 1991. *Atmospheric Chemistry and Physics*, *15*(8), 4215–4224. https://doi.org/10.5194/acp-15-4215-2015

Osprey, S. M., Butchart, N., Knight, J. R., Scaife, A. A., Hamilton, K., Anstey, J. A., et al. (2016). An unexpected disruption of the atmospheric Quasi-Biennial Oscillation. *Science*, *353*(6306), 1424–1427. https://doi.org/10.1126/science.aah4156

Petropavlovskikh, I., Godin-Beekmann, S., Hubert, D., Damadeo, R., Hassler, B., & Sofieva, V. (Eds.) (2019). SPARC/IO3C/GAW report on long-term ozone trends and uncertainties in the stratosphere. SPARC Report No. 9. GAW Report No. 241, WCRP-17/2018. https://doi.org/10.17874/f899e57a20b

Ploeger, F., & Garny, H. (2022). Hemispheric asymmetries in recent changes in the stratospheric circulation. *Atmospheric Chemistry and Physics*, *22*(8), 5559–5576. https://doi.org/10.5194/acp-22-5559-2022

Richter, J. H., Butchart, N., Kawatani, Y., Bushell, A. C., Holt, L., Serva, F., et al. (2020). Response of the Quasi-Biennial Oscillation to a warming climate in global climate models. *Quarterly Journal of the Royal Meteorological Society*, *148*(744), 1490–1518. https://doi.org/10.1002/qj.3749

Rosenfield, J. E., & Douglass, A. R. (1998). Doubled $CO_2$ effects on $NO_y$ in a coupled 2D model. *Geophysical Research Letters*, *25*(23), 4381–4384. https://doi.org/10.1029/1998gl900147

Shepherd, T. G., & Jonsson, A. I. (2008). On the attribution of stratospheric ozone and temperature changes to changes in ozone-depleting substances and well-mixed greenhouse gases. *Atmospheric Chemistry and Physics*, *8*(5), 1435–1444. https://doi.org/10.5194/acp-8-1435-2008

Sofieva, V. F., Szelag, M., Tamminen, J., Kyrola, E., Degenstein, D., Roth, C., et al. (2021). Measurement report: Regional trends of stratospheric ozone evaluated using the MErged GRIdded Dataset of Ozone Profiles (MEGRIDOP). *Atmospheric Chemistry and Physics*, *21*(9), 6707–6720. https://doi.org/10.5194/acp-21-6707-2021

Steinbrecht, W., Froidevaux, L., Fuller, R., Wang, R., Anderson, J., Roth, C., et al. (2017). An update on ozone profile trends for the period 2000 to 2016. *Atmospheric Chemistry and Physics*, *17*, 10675–10690. https://doi.org/10.5194/acp-17-10675-2017

Strahan, S. E., Douglass, A. R., & Newman, P. A. (2013). The contributions of chemistry and transport to low Arctic ozone in March 2011 derived from Aura MLS observations. *Journal of Geophysical Research: Atmospheres*, *118*(3), 1563–1576. https://doi.org/10.1002/jgrd.50181

Zawodny, J. M., & McCormick, M. P. (1991). Stratospheric Aerosol and Gas Experiment II measurements of the Quasi-Biennial Oscillations in ozone and nitrogen dioxide. *Journal of Geophysical Research*, *96*(D5), 9371–9377. https://doi.org/10.1029/91jd00517